

# Supplementary Information to Quantum Risk Analysis

Stefan Woerner<sup>1,\*</sup> and Daniel J. Egger<sup>1</sup>

<sup>1</sup>IBM Research – Zurich

(Dated: January 25, 2019)

## A. Financial concepts

In this section we provide a short introduction to some of financial concepts referred to throughout the main text. We start with a short introduction on bonds. A bond is a contract between two parties. The bond buyer pays the bond issuer the price  $P$  of the bond. In exchange, the bond issuer is contractually obliged to provide future payments to the bond buyer. Throughout the life of the bond, the issuer makes regular coupon payments, of an amount  $C$ , to the bond holder. (A bond that pays no coupon is called a *zero coupon bond*.) When the bond matures, at time  $T$  after the issuance date, the issuer pays to the bond holder a final sum named the face value  $F$  of the bond. The duration  $T$  is the maturity of the bond and the *coupon rate*  $c$  is given by  $C = cF$ . If the bond buyer holds the bond until maturity his return is the *yield to maturity*  $YTM$

$$P = \sum_{i=1}^n \frac{C}{(1 + YTM)^i} + \frac{F}{(1 + YTM)^n}.$$

The yield of bonds plotted as function of the time remaining until they mature results in a curve called the *yield curve*.

## B. Amplitude estimation

In this section, we introduce the *amplitude estimation* (AE) algorithm.

Suppose a unitary operator  $\mathcal{A}$  acting on a register of  $(n + 1)$  qubits such that  $\mathcal{A}|0\rangle_{n+1} = \sqrt{1-a}|\psi_0\rangle_n|0\rangle + \sqrt{a}|\psi_1\rangle_n|1\rangle$  for some normalized states  $|\psi_0\rangle_n$  and  $|\psi_1\rangle_n$ , where  $a \in [0, 1]$  is unknown. AE allows the efficient estimation of  $a$ , i.e., the probability of measuring  $|1\rangle$  in the last qubit [1]. This is done using an operator  $Q$  defined as

$$Q = \mathcal{A}(\mathbb{I} - 2|0\rangle_{n+1}\langle 0|_{n+1})\mathcal{A}^\dagger (\mathbb{I} - 2|\psi_0\rangle_n\langle 0|_n|\psi_0\rangle_n\langle 0|),$$

where  $\mathbb{I}$  denotes the identity operator, and Quantum Phase Estimation [2] to approximate certain eigenvalues of  $Q$ .

If  $n = 0$ , as e.g. considered in the Section *T-Bill on a single period binomial tree* in the main text, the reflections defining  $Q$  reduce to the Pauli  $Z$ -operators and  $Q$  simplifies to  $\mathcal{A}Z\mathcal{A}^\dagger Z$ . In addition, if  $\mathcal{A} = R_y(\theta)$  then it can be easily seen that  $Q = R_y(2\theta)$ .

AE requires  $m$  additional qubits and  $M = 2^m$  (controlled) applications of  $Q$ . The  $m$  qubits are first put into equal superposition by applying Hadamard gates. Then, they are used to control different powers of  $Q$ . And last, after an inverse Quantum Fourier Transform has been applied, their state is measured, see the circuit in Fig. 1.

This results in an integer  $y \in \{0, \dots, M - 1\}$ , which is classically mapped to the estimator  $\tilde{a} = \sin^2(y\pi/M) \in [0, 1]$ . The estimator  $\tilde{a}$  satisfies

$$\begin{aligned} |a - \tilde{a}| &\leq \frac{2\sqrt{a(1-a)}\pi}{M} + \frac{\pi^2}{M^2} \\ &\leq \frac{\pi}{M} + \frac{\pi^2}{M^2} = O(M^{-1}), \end{aligned} \quad (1)$$

with probability of at least  $\frac{8}{\pi^2}$ . This represents a quadratic speedup compared to the  $O(M^{-1/2})$  convergence rate of classical Monte Carlo methods [3].

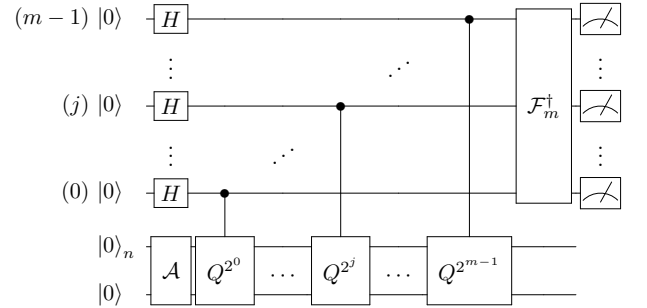


FIG. 1: Quantum circuit for amplitude estimation as introduced in [1].  $H$  is the Hadamard gate and  $\mathcal{F}_m^\dagger$  denotes the inverse Quantum Fourier Transform on  $m$  qubits.

## C. CVaR error bound

Since  $\mathbb{P}[X \leq l_\alpha]$  is replaced by an estimation, we cannot directly apply the AE error bound for CVaR. Assume two unknowns  $A, B > 0$  and their estimates  $\tilde{A} = A + \delta_a$ ,  $\tilde{B} = B + \delta_b > 0$ , where  $|\delta_a|, |\delta_b| \leq \delta$  for  $\delta > 0$ . The first order Taylor approximation of  $\frac{A}{B} - \frac{\tilde{A}}{\tilde{B}}$  with respect to  $\delta_a$

\*Electronic address: wor@zurich.ibm.com

and  $\delta_b$  around zero can be used to derive

$$\left| \frac{A}{B} - \frac{\tilde{A}}{\tilde{B}} \right| \leq \frac{1}{B} \left| \delta_a - \frac{A}{B} \delta_b \right| \leq \frac{1}{B} \left( 1 + \frac{A}{B} \right) \delta,$$

where we ignore higher order terms of  $\delta_a$  and  $\delta_b$ .

Setting  $\frac{A}{B} = \frac{1}{l_\alpha} \text{CVaR}_\alpha(X)$  and  $B = \mathbb{P}[X \leq l_\alpha]$ , multiplying everything with  $l_\alpha$  and replacing  $\delta$  by  $\frac{\pi}{M}$  leads to the following bound for the approximation error  $\epsilon > 0$  of  $\text{CVaR}_\alpha(X)$ :

$$\begin{aligned} \epsilon &\leq \frac{l_\alpha + \text{CVaR}_\alpha(X)}{\mathbb{P}[X \leq l_\alpha]} \frac{\pi}{M} \\ &\approx \frac{\text{VaR}_\alpha(X) + \text{CVaR}_\alpha(X)}{1 - \alpha} \frac{\pi}{M}, \end{aligned}$$

where again we omit higher order terms. Thus, the quantum estimation of CVaR also achieves a quadratic speedup compared to classical Monte Carlo methods.

#### D. Creating circuits that implement polynomials, an example

Fig. 2 shows an example circuit for a polynomial mapping applied to an ancilla qubit.

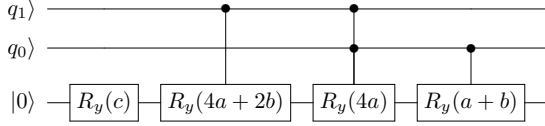


FIG. 2: Quantum circuit realizing the mapping  $|x\rangle_n |0\rangle \mapsto |x\rangle_n (\cos(\zeta(x)/2) |0\rangle + \sin(\zeta(x)/2) |1\rangle)$  for  $\zeta(x) = ax^2 + bx + c$  and  $x \in \{0, 1, 2, 3\}$ . Exploiting  $x = 2q_1 + q_0$  and  $q_i^2 = q_i$  leads to  $\zeta(x) = (4a + 2b)q_1 + 4aq_0q_1 + (a + b)q_0 + c$ , which can be directly mapped to a circuit.  $R_y$  denotes a Y-rotation.

#### E. Error bound for $F$ approximation

Suppose  $\zeta(y)$  denotes the Taylor approximation of Eq. 7 in the main text. of order  $(2u + 1)$ . Then, the error bound is derived from the next coefficient in the Taylor series (plus higher order terms). Therefore, we analyze the Taylor series

$$\begin{aligned} &\sin^{-1} \left( \sqrt{y + \frac{1}{2}} \right) \\ &= \frac{\pi}{4} + \sum_{u=0}^{\infty} \left( \prod_{i=1}^u (2i - 1) \right) \frac{2^u}{(2u + 1)u!} y^{2u+1}, \end{aligned}$$

for  $y \in [-\frac{1}{2}, +\frac{1}{2}]$ . The Taylor series can be derived by first taking the derivative, using the corresponding Taylor series, and integrating the different terms independently. Replacing  $y$  by  $cy$  for  $c \in (0, 1]$  and the fact that the

extreme values are assumed for  $y = \pm \frac{1}{2}$  leads to a bound on the individual terms for a particular  $u$  given by

$$\left( \prod_{i=1}^u (2i - 1) \right) \frac{2^u}{(2u + 1)2^{2u+1}u!} c^{2u+1} \leq \frac{c^{2u+1}}{2(2u + 1)},$$

where we used  $\prod_{i=1}^u (2i - 1) \leq 2^u u!$ . For a Taylor approximation of order  $2u + 1$ , the error bound is given by the bound on the next Taylor coefficient in the series, i.e. for  $2u + 3$ .

#### F. Topology of IBM Q 5 Yorktown and IBM Q 20 Tokyo quantum processor

Figures 3 and 4 show the topologies of the IBM Q 5 Yorktown [4] and IBM Q 20 Tokyo [5] quantum processors. The lines indicate the connectivity, i.e., the pairs of qubits that allow the application of CNOT gates.

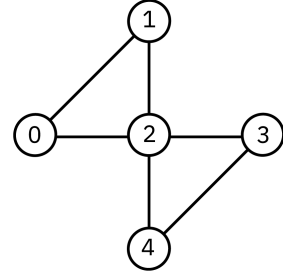


FIG. 3: Topology of IBM Q 5 Yorktown quantum processor.

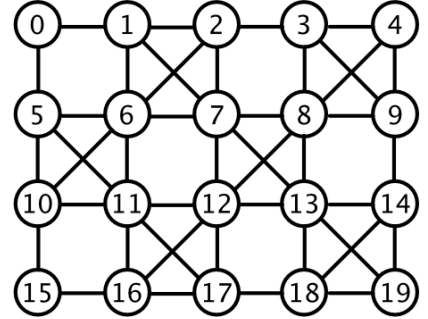


FIG. 4: Topology of IBM Q 20 Tokyo quantum processor.

#### G. $U_2, U_3$ single qubit rotations

In the following, we define the single qubit rotations,  $U_2, U_3$ , used in Fig. 1 in the main text, and defined e.g. in [6]:

$$\begin{aligned} U_2(\phi, \lambda) &= \begin{pmatrix} 1/\sqrt{2} & -e^{i\lambda}/\sqrt{2} \\ e^{i\phi}/\sqrt{2} & e^{i\lambda+i\phi}/\sqrt{2} \end{pmatrix} \\ U_3(\theta, \phi, \lambda) &= \begin{pmatrix} \cos(\theta/2) & -e^{i\lambda} \sin(\theta/2) \\ e^{i\phi} \sin(\theta/2) & e^{i\lambda+i\phi} \cos(\theta/2) \end{pmatrix}. \end{aligned}$$

## H. Convergence Analysis

For the Monte Carlo simulation we consider a 95%-confidence interval. To enable a fair comparison despite the small number of samples, we compute an optimistic bound and assume the exact standard error  $\sqrt{p(1-p)}$ , where  $p$  denotes the success probability of the Bernoulli random variable. For  $p = 0.3$  and a 95% confidence level, the resulting confidence interval is given by  $[0.3 - 0.898/\sqrt{M}, 0.3 + 0.898/\sqrt{M}]$ .

For the quantum algorithm we exploit the error bound given in Eq. 1. Although the exact value of  $p$  is supposed

to be unknown, we can use the estimated value  $\tilde{a}$  to compute an error bound. The algorithm results in an integer  $y$  which is classically mapped to  $\tilde{a} = \sin^2(y\pi/M)$ , and we assume  $y$  is the most probable result of the quantum algorithm. The theory says that for  $\theta_a$ , defined through  $a = \sin^2(\theta_a)$ , it holds that  $\theta_a \in [(y-1)\pi/M, (y+1)\pi/M]$ . Then, the interval for  $\theta_a$  can be mapped to an interval for  $a$ , whose width is compared to the confidence interval from the Monte Carlo simulation. Since the mapping from  $y$  to  $a$  is non-linear, the error bound is not symmetric around  $\tilde{a}$  and we consider the maximum.

- 
- [1] G. Brassard, P. Hoyer, M. Mosca, and A. Tapp, *Contemporary Mathematics* **305** (2002), URL <http://dx.doi.org/10.1090/conm/305>.
  - [2] A. Y. Kitaev (1995), arXiv:9511026.
  - [3] P. Glasserman, P. Heidelberger, and P. Shahabuddin, in *Mastering Risk* (2000), vol. 2, pp. 5–18.
  - [4] *IBM Q 5 Yorktown*, <https://github.com/QISKit/qiskit-backend-information/blob/master/backends/yorktown/V1/README.md>, accessed: 2018-05-22.
  - [5] *IBM Q 20 Tokyo*, <https://quantumexperience.ng.bluemix.net/qx/devices>, accessed: 2018-05-22.
  - [6] *Qiskit* (2019), URL <https://qiskit.org/>.